Hindawi Publishing Corporation
Mathematical Problems in Engineering
Volume 2014, Article ID 518120, 13 pages
http://dx.doi.org/10.1155/2014/518120

Research Article

Route Assessment for Unmanned Aerial Vehicle Based on Cloud Model

Xixia Sun, Chao Cai, Jie Yang, and Xubang Shen

State Key Laboratory for Multispectral Information Processing Technologies, School of Automation, Huazhong University of Science and Technology, Wuhan, Hubei 430074, China

Correspondence should be addressed to Chao Cai; caichao@hust.edu.cn

Received 6 January 2014; Revised 27 April 2014; Accepted 28 April 2014; Published 29 December 2014

Academic Editor: Balaji Raghavan

An integrated route assessment approach based on cloud model is proposed in this paper, where various sources of uncertainties are well kept and modeled by cloud theory. Firstly, a systemic criteria framework incorporating models for scoring subcriteria is developed. Then, the cloud model is introduced to represent linguistic variables, and survivability probability histogram of each route is converted into normal clouds by cloud transformation, enabling both randomness and fuzziness in the assessment environment to be managed simultaneously. Finally, a new way to measure the similarity between two normal clouds satisfying reflexivity, symmetry, transitivity, and overlapping is proposed. Experimental results demonstrate that the proposed route assessment approach outperforms fuzzy logic based assessment approach with regard to feasibility, reliability, and consistency with human thinking.

1. Introduction

Unmanned aerial vehicles (UAVs) are aircrafts without onboard pilots that can be remotely controlled or can fly autonomously based on preplanned flight routes, increasingly being used in real-world applications [1]. Such a preplanned flight route is usually automatically provided by a route planner based on a cost function [2]. However, in some cases, the predetermined cost function cannot account for all potential external conditions and, therefore, the optimal or near-optimal route provided by the route planner may not represent a desirable solution for many mission scenarios and could result in erroneous decision support [3]. An effective way to handle these issues is multiroute planning, where several candidate routes are preplanned, and in real applications, a suitable route is chosen from these alternative routes based on mission characteristics [4, 5]. Therefore, decision making among alternative routes for UAVs is required in real applications.

Overall performance of a route usually consists of two parts: route length and route risk. However, a flight route is complex and is characterized by various features: distance traveled, fuel consumption, radar exposure, smoothness, and so forth. Therefore, there are multiple research studies incorporating other assessment criteria such as smoothness and average altitude into their definitions of route performance [6, 7]. However, owing to the complexity of the UAV route assessment problem, some of the criteria considered may not be sufficient enough to explain the complex interactions among various factors affecting overall route performance. As such, a systematic and transparent assessment framework is required to guide assessment process, which should contain features describing multiple conflicting criteria as well as representing dynamics and uncertainties in decision environment.

Trade-offs among route assessment criteria are characterized by weight parameters assigned by human experts. Actually, in complex situations, experiences and preferences of humans are represented by linguistic and vague patterns. One way to capture the meanings of linguistic variables is to use the fuzzy logic approach to associate each linguistic term with a possibility distribution [8]. In previous research concerning route assessment, weights of criteria are usually deterministic representations [2–7], which typically do not contain descriptions of various sources of uncertainties. Several studies tried to account for linguistic uncertainty

and ambiguity elements in route assessment decisions based on type-1 fuzzy sets (T1 FSs) [9, 10]. However, type-1 fuzzy set theory only considers fuzziness of membership grade and does not take randomness into consideration. Therefore, some new theoretical methods are required for dealing with both fuzziness and randomness existing in human knowledge.

Cloud model [11] proposed by Li et al. is based on fuzzy theory and probability statistics, which integrates fuzziness and randomness to constitute the mapping between qualitative knowledge description and quantitative value expression. Therefore, it overcomes the subjective randomness in fuzzy membership grade when being determined. Since its introduction, cloud theory is well developed and many techniques based on the cloud model are proposed, such as normal cloud generator, normal cloud transformation, cloud operation, and uncertainty reasoning [12]. Owing to the complexity of the route assessment problem and human cognition incompleteness, there are a large number of uncertainties such as fuzziness and randomness in human knowledge and perceptions. Cloud model, as a model of the uncertainty transformation between quantitative knowledge representation and qualitative concept, can reflect the uncertainties of things in the universe and the concepts in human knowledge due to its good mathematical properties. To model and deal with various kinds of uncertainties in the decision environment, an integrated route assessment approach based on cloud model is proposed in this study. Recently, cloud model has been successfully applied to various domains, such as intelligent algorithm improvement [13, 14], risk assessment [15], and image processing [16].

In this paper, factors that have significant effects on route assessment operations were identified and a hierarchical criteria framework was built. A comprehensive route assessment approach based on cloud model was proposed to cope with various sources and kinds of uncertainties existing in the assessment environment, where words were modeled by normal clouds and each estimated survivability probability histogram provided by Monte Carlo simulations was converted into normal clouds. Cloud arithmetic operations were performed to obtain overall scores of candidate routes, enabling different kinds of uncertainties existing in the data to be effectively preserved and propagated into the final results.

An outline of the rest of this paper is as follows. Section 2 provides brief descriptions of the proposed route assessment method, the battlefield environment modeling, and the proposed hierarchical criteria framework. Details of assessment criteria's calculation models are presented in Section 3. The proposed route assessment method based on cloud model is described in detail in Section 4 and experimental results are given in Section 5. Finally, the paper is concluded in Section 6.

2. Route Assessment Problem Modeling

2.1. General Assessment Framework. Route assessment and selection problems confronted by decision-makers require aggregation of preferences over multiple assessment criteria.

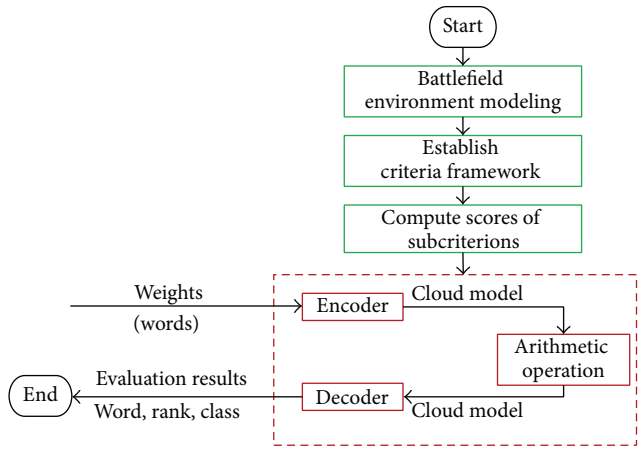

Figure 1: Establishment process for the proposed UAV route assessment approach based on cloud model.

Assessment must not focus only on the UAV's mission performance, but also on its ability to survive a wide variety of threats and situations at an affordable fuel cost and safety level. Therefore, route assessment can be addressed in the multi-criteria decision making (MCDM) framework, where several criteria like length, mission performance, smoothness, and risk need to be weighed against each other. Criteria scores are computed based on their mathematical models, and trades-offs among criteria are determined by weight factors supplied by military experts.

As mentioned previously, various kinds and sources of uncertainties such as randomness and fuzziness exist in the assessment environment [17]. Random parameters like pop-up threats and actions of the enemy make survivability of a route uncertain. To deal with these random factors and embed them in the final decision, survivability of a route is represented by survivability probability histogram. Preferences and judgments of military experts are linguistic and fuzzy in nature, which are handled via cloud model. To take these different kinds of uncertainties into account within the same assessment framework, each survivability probability histogram is converted into membership clouds by cloud transformation [18]. The assessment procedure of this study (see Figure 1) is as follows and the following parts provide detailed descriptions of each step.

Step 1. Model battlefield environment, including terrain, no-fly zones, and threats.

Step 2. Select criterions for UAV route assessment and establish the hierarchical criteria framework.

Step 3. Compute the numerical score of each individual subcriterion. Particularly, use Monte Carlo simulations and Markov chain to estimate survivability probability density function.

Step 4. Model linguistic terms using normal clouds and specify the fuzzy weights of each individual criterion and subcriterion using linguistic terms (encoder).

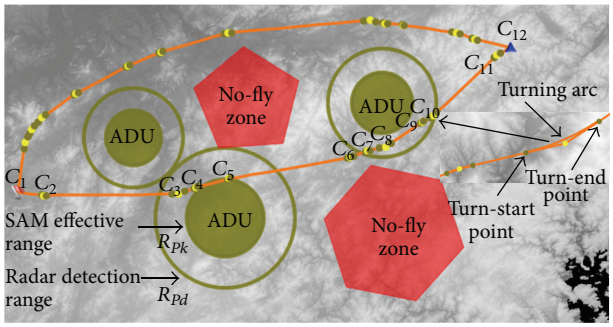

Figure 2: Typical UAV battlefield model.

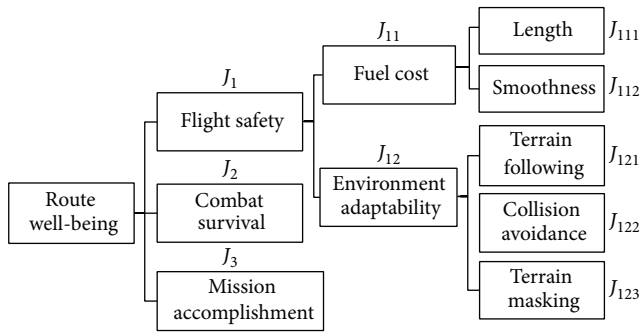

Figure 3: The hierarchical structure of route assessment criteria.

Step 5. Map score of each subcriterion into a specific normal cloud and compute the total value of each individual route by using the fuzzy weights and criterion rating matrix.

Step 6. Score and rank alternative routes' overall performance (decoder).

2.2. Battlefield Environment Modeling. Here, we consider combat situations between the UAV and its opponent forces. The battlefield is a geographical area and the airspace above it. On the terrain map, there are certain no-fly zones represented by polygon regions that the UAV must not enter. Particularly, in a typical battlefield environment, several opponent sensor platforms are deployed. This study focuses on integrated air defense system consisting of Air Defense Units (ADUs) that are groups of radars and surface-to-air missile (SAM) sites, whose proposes are to detect, track, and, if necessary, destroy the UAV. In Figure 2, circles placed on the map in various positions are four ADUs. The inner circles represent the boundaries of relative risk ranges of the SAMs, while the radii of the outer circles represent the maximum detection distances of the radars. Before candidate routes are evaluated and ranked, threats information is collected, including locations, radar detection ranges, radar model coefficients, and SAM effective ranges. These perceived threats located on the ground or sea are categorized as deterministic.

The flyable vehicle routes are Dubins curves in this study. As depicted in Figure 2, the two curves between the start and destination positions are candidate routes to be ranked. In this research, the mission that the UAV is performing is defined as "air-to-ground attacking mission" (strike). The sortie mission starts with takeoff from the start position, during the mission, UAV follows a preplanned route, passing through air defense network and preserving its survival before a follow-on ground attack of high value targets. When the UAV reaches its self-control terminal point which is a predefined waypoint near the target, the self-guidance phase begins, and the sensor fixed on the UAV starts searching potential targets in a predefined area, as the searching mission is performed, the UAV executes its prearranged attacking mission.

Note that, in performing a real mission, it is hard to know all information of the combat environment in advance. In many cases, maybe threats occur randomly in the battlefield. In previous studies, it is often assumed that pop-up threats appear with predetermined probabilities during the flight [4, 19]. However, such probabilities may be of limited representations of battlefield scenarios. In many scenarios, the appearance probability of one pop-up threat at a location might depend on the appearances of other pop-up threats at various previous locations. To model battlefield realistically, the randomness of other pop-up threat appearance is quantified via a Markov model [20] in this study.

2.3. Select Criteria for Decision Making. Based on schulte's goal model [21] that a pilot has when selecting a route, specifically, we determine the critical factors that affect route performance and develop a systemic and hierarchical criteria framework, constructed in terms of three main aspects (see Figure 3): flight safety, combat survival, and mission accomplishment. Flight safety includes objectives concerning safe flying of the UAV and, therefore, needs to consider factors such as terrain, fuel level, and no-fly zones in the battlefield. Combat survival is defined as the capability of the UAV to avoid and/or withstand the hostile forces when flying along the route. Mission accomplishment describes performance of the mission.

Kinds of factors affect flight safety and they are decomposed into specific items: fuel cost and environment adaptability. Two primary factors affect fuel consumption of a route: route length and route smoothness. Generally, the longer the route, the more fuel a UAV needs. At the same time, in view of the physical limitation and the fuel limit of the UAV, it usually does not wish to turn or climb/dive frequently. When route performance in terms of environment adaptability is evaluated, compromises must be made: the higher the UAV flies above the ground, the lower probability of colliding with the terrain or obstacle it has; however, it may pose itself to a greater chance of getting detected by enemy forces. To take into account all these route features influenced by battlefield environment, route environment adaptability composes of three subcriterions: the abilities of terrain following, terrain/obstacle collision avoidance, and terrain masking. The following section describes mathematical models of these criterions and subcriterions.

3. Models for Scoring Criteria and Subcriteria

3.1. Flight Safety. As mentioned previously, each UAV route Z is a Dubins route in this research, described as a sequence of nodes in the three-dimensional (3-D) space:

$$Z = (C_1, C_2, \ldots, C_M), \tag{1}$$

where C_1 and C_M are the start node and the destination node, respectively, and M is the number of route nodes. Each path node C_i is specified by the 3D coordinates (x_i, y_i, z_i) of the intersection point between line segments $\overrightarrow{C_{i-1}C_i}$ and $\overrightarrow{C_iC_{i+1}}$. Each pair of adjacent line segments $\overrightarrow{C_{i-1}C_i}$ and $\overrightarrow{C_iC_{i+1}}$ is connected by a circular arc satisfying UAV dynamics constraints.

Route length $J_{111}(Z)$ represents the total length of all line segments and turning circular arcs. Let L_i and l_i denote lengths of the ith line segment and turning arc, respectively. $J_{111}(Z)$ is expressed as

$$J_{111}(Z) = \sum_{i=1}^{M-1} (L_i + l_i). \tag{2}$$

Take two adjacent line segments $\overrightarrow{C_{i-1}C_i}$ and $\overrightarrow{C_iC_{i+1}}$, for example; assume that C'_{i-1}, C'_i, and C'_{i+1} are the corresponding projections of route nodes C_{i-1}, C_i, and C_{i+1} in the xoy plane, respectively. The turn angle at node C_i is defined as the angle difference between two adjacent edges $\overrightarrow{C'_{i-1}C'_i}$ and $\overrightarrow{C'_iC'_{i+1}}$. Similarly, the climb/dive angle of route segment $\overrightarrow{C_iC_{i+1}}$ is defined as the angle between route segment $\overrightarrow{C_iC_{i+1}}$ and its projection in the horizontal plane.

Let (x_i, y_i, z_i) and $(x_{i+1}, y_{i+1}, z_{i+1})$ denote the 3D coordinates of nodes C_i and C_{i+1}, respectively. Route smoothness concerns the turn rate F_i and climb/dive rate S_i at each node C_i, as the following expressions.

(1) The turn rate F_i at node C_i is expressed as

$$F_i = \frac{\arccos\left(\left(\overrightarrow{C'_{i-1}C'_i} \cdot \overrightarrow{C'_iC'_{i+1}}\right) / \left(\left\|\overrightarrow{C'_{i-1}C'_i}\right\| \left\|\overrightarrow{C'_iC'_{i+1}}\right\|\right)\right)}{\alpha_{\max}}, \tag{3}$$

where $\alpha_{\max}$ is the maximum turn angle.

(2) When the UAV is climbing/diving along route segment $\overrightarrow{C'_iC'_{i+1}}$, the climb/dive rate S_i at node C_i is defined as

$$S_i = \frac{\arctan\left(\left|z_{i+1} - z_i\right| / \sqrt{(x_{i+1} - x_i)^2 + (y_{i+1} - y_i)^2}\right)}{\beta_{\max}}, \tag{4}$$

where $\beta_{\max}$ is the maximum climb/dive angle. Smoothness $J_{112}(Z)$ is defined as the sum of route nodes' turn rate and climb/dive rate:

$$J_{112}(Z) = \sum_{i=1}^{M-1} (F_i + S_i). \tag{5}$$

Route performance regarding environment adaptability is determined by specific battlefield scenarios, such as terrain and no-fly zones. It is difficult to analytically estimate their impacts on route performance. To facilitate computations, a route is discretized into N sample points with equal length step ΔR. Assume that the UAV flies at a constant speed. Environment adaptability of a route is evaluated based on these discretized sections.

(1) Terrain Following. Terrain following flight requires the UAVs to maintain a minimum preselected clearance above a given terrain to minimize the probability of being detected or tracked. Kinds of measures of terrain following ability of a route have been discussed [22, 23]. In this research, the terrain following ability is defined as

$$J_{121}(Z) = \frac{1}{N}\sum_{i=1}^{N} {e_i}^2, \tag{6}$$

where e_i represents the closeness of the altitude of ith sample point to the underlying terrain, defined as: $e_i = z_i - T_i - C_{\min}$, where z_i is the altitude of ith sample point, T_i is the terrain elevation at point (x_i, y_i), and $C_{\min}$ is minimum ground clearance. A smaller $J_{121}(Z)$ means a better terrain following path.

(2) Terrain/Obstacle Collision Avoidance. UAVs flying at low altitude will have the risk of collision with terrain or obstacles. In addition, the UAV is not allowed to enter any no-fly zones. Several terrain/obstacle collision avoidance measures have been discussed [24–27]. However, these measures were under some assumptions and focused only on selected factors, which were often reductionist in nature. In this study, the capacity of the UAV to avoid terrain/obstacle collision is considered as a stochastic model based on stochastic processes, and a terrain/obstacle collision avoidance measure $J_{122}(Z)$ is proposed. This measure takes the uncertainty regarding the actual flight route the UAV travels into account, which can be used to estimate the probability that the UAV collides with terrain/obstacle along the route. $J_{122}(Z)$ is formulated as

$$\begin{aligned} J_{122}(Z) &= \exp\left(-\Delta t \sum_{i=1}^{N} f_i\right) \\ \text{Where } f_i &= \frac{1}{\sqrt{2\pi}\sigma} \int_{-\infty}^{T_i} \exp\left(-\frac{(h - z_i)^2}{2\sigma^2}\right) dh, \end{aligned} \tag{7}$$

where Δt is the UAV flying time from point i to $i + 1$. T_i is the height of terrain at point i. h representing the vehicle real flying altitude at point i follows a normal distribution $N(z_i, \sigma, h)$ in height direction, where z_i is the expectation altitude at point i, and σ is the stand deviation. As Figure 4 illustrates, f_i states the instantaneous probability of collision with the terrain at point i. A larger $J_{122}(Z)$ implies that the UAV crosses fewer obstacles.

(3) Terrain Masking. UAVs flying at low altitude can benefit from the terrain-masking effect that will help them to avoid radar detection, especially unknown radars [2]. The following

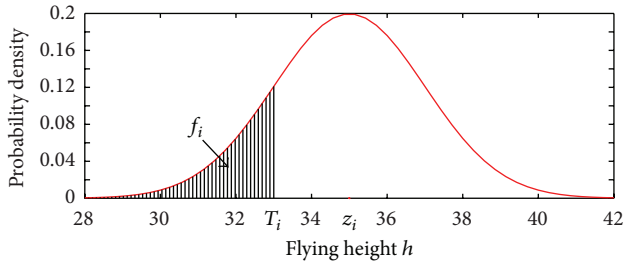

FIGURE 4: Vehicle flying height distribution at the ith point of the route. f_i is equal to the area of the shaded region in the figure, representing the instantaneous probability that the UAV collides with terrain or obstacle at point i.

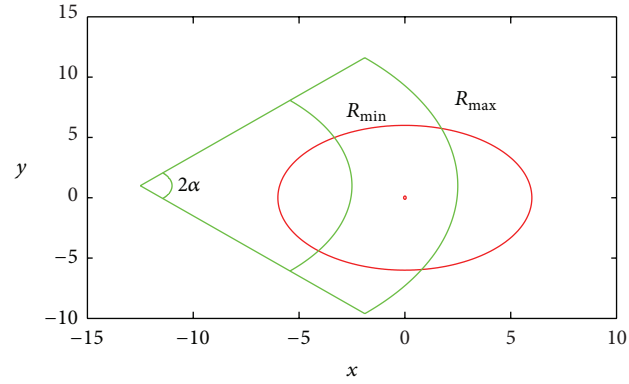

FIGURE 5: Target area at the terminal search time. The region inside the ellipse represents the potential target area, and the sector is the FOV of the sensor equipped on the UAV.

expression $J_{123}(Z)$ calculates this value of object, which is the average altitude of the N discrete points. A smaller $J_{123}(Z)$ indicates a higher terrain masking path:

$$J_{123}(Z) = \frac{1}{N}\sum_{i=1}^{N} z_i. \tag{8}$$

3.2. Modeling the Survivability of a Route. Same as that in [28], survivability of a UAV flying along a preplanned route is considered as a stochastic model based on stochastic processes. In this model, the survival function is described by

$$R(t) = P(T_{\text{hit}} > t) = \exp\left(-\int_0^t \lambda(u)\, du\right), \tag{9}$$

where $\lambda(u)$ is defined as the intensity or hit rate. Under the assumptions that hit rates were functions of the distance from the UAV to threat center, three models of hit rate were suggested in [28] and analytical expressions were provided. Without loss of generality, we adopt the constant threat model in this study; that is, $\lambda(u) = \lambda_0$.

Let t_f denote the time required to fly the entire route, let M denote the number of ADUs, let v denote the speed of the UAV, and let d_i denote length of the route segment that is in the effective range of the ith SAM. According to formula (9), assessment of combat survival is equal to survivability of the UAV at time instance t_f (i.e., survivability of a route), expressed as

$$J_2(Z) = P\left(T_{\text{hit}} > t_f\right) = \exp\left(-\frac{\lambda_0}{v}\sum_{i=1}^{M} d_i\right). \tag{10}$$

Note that survivability model requires information about threats that are located on or near the route. However, as mentioned previously, threats could appear randomly during the flight. Therefore, survivability of a route is also a random variable, and analytical estimates for survivability distribution function are difficult to obtain. In view of this problem, Monte Carlo simulations are applied to estimate survivability probability density function and investigate how random uncertainty affects survivability in this study.

Each Monte Carlo simulation consists of a flight of the UAV from the start position following the mission route, during which several pop-up threats appear randomly via Markov chain. At the end of each simulation, survivability for that simulation is stored, and all simulations are summarized into a histogram that can be further used to estimate the probability density function of survivability.

3.3. Mission Accomplishment. The exact position of the target to be attacked maybe unknown previously, and we know its priori probability density function $h(x, y)$. When the UAV reaches its auto control terminal point, the sensor equipped on the UAV is activated and scans the potential target area to find the hostile target. In this research, mission accomplishment is measured by search probability, meaning the probability that the target can be found when sensor is activated.

The instantaneous sensing region of the sensor on the ground, known as the field of view (FOV) specified by the distance and the deviation angle, is modeled as a sector (see Figure 5) in this research. The azimuth search range and distance search range of the FOV are $\pm\alpha$ and $[R_{\min}, R_{\max}]$, respectively. Let B denote the set of all points in the potential target area that the seeker can scan and assume that as long as the search region covers the target, the sensor can detect the target and the probability that detects a target that lies outside of the sensor's FOV is zero. Therefore, the general detection function $J_3(Z)$ describing the assessment of mission accomplishment is estimated as follows:

$$J_3(Z) = \iint_B h(x, y)\, dx\, dy. \tag{11}$$

Once the score of each subcriterion is calculated, the following step is selecting a set of suitable weight coefficients. To effectively represent linguistic terms of military experts, we introduce to adopt cloud model to handle various uncertainties. Details of cloud model and its applications in the UAV route assessment are discussed below.

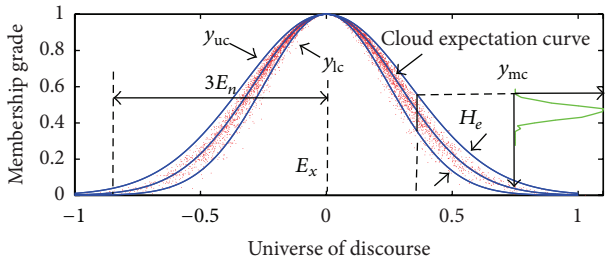

Figure 6: Membership cloud of "about zero" $(0, 1/3, 0.03)$. y_{uc} and y_{lc} are upper and lower cloud curve, respectively. y_{mc} is the cloud expectation curve.

4. Ranking Routes Using Cloud Model

4.1. Cloud Model. Cloud is a model to address the relationship between randomness and fuzziness for qualitative concepts and quantitative values, defined as follows.

Suppose that T is a language value of domain U, and mapping $C_T(x) : U \to [0, 1], \forall x \in U, x \to C_T(x)$. Then, the distribution of $C_T(x)$ in U is called the membership cloud of T, or cloud in short, and each projection is called a cloud drop in the distribution. If distribution of $C_T(x)$ is normal, it is named normal cloud.

Normal cloud model employs expectation E_x, entropy E_n, and super entropy H_e to represent qualitative concept. As Figure 6 depicts, E_x determines the center of the cloud. E_n is the uncertainty measurement of the qualitative concept, decided by the randomness and the fuzziness of the concept. H_e is the uncertainty measurement of the entropy, reflecting cloud drops' dispersive degree. For example, a normal cloud $(0, 1/3, 0.03)$ representing a linguistic term "about zero" is shown in Figure 6.

From the view of fuzzy set theory, normal cloud is similar to Gaussian interval type-2 fuzzy set (IT2 FS) with uncertainty standard variance σ [18]. According to the "$3E_n$ principle," 99.7% of cloud drops are bounded by the upper cloud curve y_{uc} and the lower cloud curve y_{lc}. y_{uc} and y_{lc} are similar to the upper and lower membership functions of the IT2 FSs, respectively, described by

$$y_{uc} = \exp\left(\frac{-(x - E_x)^2}{2(E_n + 3H_e)^2}\right),$$
$$y_{lc} = \exp\left(\frac{-(x - E_x)^2}{2(E_n - 3H_e)^2}\right). \quad (12)$$

4.2. Words Modeling and Cloud Transformation. Linguistic weights of human experts are distinguished by five scales, which are "Very Unimportant" (VU), "Medium Unimportant" (MU), "Important" (I), "Medium Important" (MI), and "Very Important" (VI). As shown in Table 1, these linguistic variables are mapped into their corresponding normal clouds (see Figure 7), represented by conversion scales $\widetilde{1}, \widetilde{3}, \widetilde{5}, \widetilde{7}$, and $\widetilde{9}$, respectively.

Table 1: Linguistic terms for representing the importance of criterions and subcriterions and their corresponding normal clouds.

Linguistic term	Fuzzy number	Normal cloud
Very Unimportant (VU)	$\widetilde{1}$	(1, 0.5, 0.05)
Medium Unimportant (MU)	$\widetilde{3}$	(3, 0.5, 0.05)
Important (I)	$\widetilde{5}$	(5, 0.5, 0.05)
Medium Important (MI)	$\widetilde{7}$	(7, 0.5, 0.05)
Very Important (VI)	$\widetilde{9}$	(9, 0.5, 0.05)

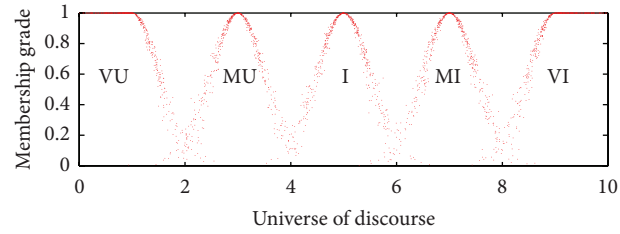

Figure 7: Membership clouds of the linguistic terms.

Several methods exist for mapping words into normal clouds [29–32], and each method has advantages and limitations. Similar to that in [29, 30], parameters of normal clouds corresponding to the linguistic scale value are established based on experiences of experts in this study. We assume that the efficient domain is $U = [0, 10]$. A subject was asked to provide the endpoints of an interval $[a_i, b_i]$ for a word on the prescribed scale $[0, 10]$, and this is done for a group of subjects. The minimum of the left endpoints and the maximum of the right endpoints are calculated; that is, $C_{\min} = \min\{a_i\}$ and $C_{\max} = \max\{b_i\}$. To the linguistic words with bilateral constraint $[C_{\min}, C_{\max}]$, we can compute the cloud parameter by the formula as follows:

$$E_x = \frac{(C_{\max} + C_{\min})}{2},$$
$$E_n = \frac{(C_{\max} - C_{\min})}{6}, \quad (13)$$
$$H_e = k,$$

where k is a constant and can be adjusted according to the fuzziness of the linguistic word. For the linguistic words "Very Unimportant" and "Very Important," their expected values reach the left boundary and the right boundary of the domain, respectively, and their corresponding clouds become half-bell clouds (shown as Figure 7).

Also, linguistic terms "Poor," "Marginal," "Adequate," "Good," and "Excellent" are used as the assessment levels to describe the performance of each route. These linguistic words are mapped into their corresponding synonyms as listed in Table 1.

Note that survivability of a route is uncertain and its probability histogram can be calculated from Monte Carlo simulations. Assessment of combat survival can be represented by expected value of survivability probability density function; however, it might not be appropriate to use such

a single value to represent how safe a route is, since it cannot represent random uncertainty existing in the battlefield and information contained in histograms is lost. To aggregate different kinds of data and keep the information contained in the histograms, it is desirable to describe score of combat survival by normal clouds. With this purpose, we convert each survivability histogram into an integration of normal clouds by cloud transformation [18]; that is,

$$\text{hist}\left(J_2(Z)\right) \longrightarrow \sum_{i=1}^{N} a_i \times C_i\left(E_{x_i}, E_{n_i}, H_{e_i}\right), \tag{14}$$

where $C_i(E_{x_i}, E_{n_i}, H_{e_i})$ $(i = 1, 2, \ldots, N)$ are normal clouds representing discrete quality concepts. a_i $(i = 1, 2, \ldots, N)$ are parameters denoting the distribution frequency of normal clouds and $\sum_{i=1}^{N} a_i = 1$. N is the number of normal clouds.

The proposed method of survivability modeling and uncertainty representation can be extended to score other criterions. For example, in real scenarios, there can be uncertainty regarding the actual flight route the UAV travels. Therefore, the location of the auto control terminal point is also random in nature, making search effectiveness of the route uncertain. With such an approach, we can estimate probability density function of route's search effectiveness and then transform the estimated probability density function into discrete concepts for further analysis.

4.3. Rank of Cloud Models. In cloud theory, arithmetic operation [33] is an operator operating on clouds; that is, given two normal clouds $C_1(E_{x_1}, E_{n_1}, H_{e_1})$ and $C_2(E_{x_2}, E_{n_2}, H_{e_2})$, the arithmetic operation result is also a normal cloud $C(E_x, E_n, H_e)$. Note that crisp numbers are considered as specific kind of clouds and all the data in the assessment framework can be mapped into normal clouds. In this research, the arithmetic operation rule is used to aggregate the criterions and subcriterions and, hence, to obtain the overall score of each route alternative.

The final score of each route is a normal cloud $\widetilde{A_i}(E_{x_i}, E_{n_i}, H_{e_i})$. The determination of the entire performance ratings of alternative routes can be based on comparing the multiple collaboration clouds with the standard assessment clouds base. Therefore, a similarity or distance measure should be used to describe the similarity between two different clouds. Several methods exist for the similarity measure between two normal clouds, and they can be classified into the following categories: (1) computer simulation methods [15, 34], which consider both fuzziness and randomness in the data but has the following difficulties: (a) they may change from experiment to experiment and require large amounts of calculations. (b) They do not satisfy reflexivity; that is, $J(C_1, C_2) \neq 1$, when $C_1 = C_2$ because the randomly generated cloud drops from C_1 and C_2 cannot always be the same. (c) They do not satisfy symmetry because of the random numbers. (2) Numerical characteristics based methods [35–37], which calculate the similarity between two normal clouds based on their differences in numerical characteristics, E_x, E_n, and H_e. These methods are easy to compute but do not consider influences of cloud drops' properties on the similarity, and the similarity between two normal clouds depends on user defined parameters. (3) Expectation curve based methods; for example, a similarity measure based on the expectation curve of two normal clouds is proposed in [38]. A problem with this approach is that it does not satisfy reflexivity; that is, when $J(C_1, C_2) = 1$, it does not necessarily imply that $C_1 = C_2$, because influence of H_e is not considered in this measure.

As shown in Figure 8, let $\overline{y_1}(x)$ ($\underline{y_1}(x)$) and $\overline{y_2}(x)$ ($\underline{y_2}(x)$) denote the upper (lower) cloud curve of normal clouds C_1 and C_2, respectively, let $\overline{S}$ ($\underline{S}$) represent the overlapping area of $\overline{y_1}(x)$ ($\underline{y_1}(x)$) and $\overline{y_2}(x)$ ($\underline{y_2}(x)$), and let $S_1 = \sqrt{2\pi}E_{n_1}$ and $S_2 = \sqrt{2\pi}E_{n_2}$ denote the area of the two normal clouds, respectively. A new similarity measure, which is based on the Jaccard similarity measure for IT2 FSs [39], is proposed in this research, calculated as

$$J\left(C_1, C_2\right) = \frac{\overline{S} + \underline{S}}{2S_1 + 2S_2 - \overline{S} - \underline{S}}. \tag{15}$$

This similarity measure satisfies reflexivity, symmetry, transitivity, and overlapping, and it utilizes both shape and thickness information of cloud drops simultaneously.

Alternative routes are ranked by comparing the numerical characteristics of their corresponding representative normal clouds [33]: the larger the value of E_{x_i}, the higher performance route A_i has; that is, if $E_{x_i} \geq E_{x_j}$, $E_{n_i} < E_{n_j}$, and $H_{e_i} < H_{e_j}$, then A_i absolutely dominates A_j; otherwise, if $E_{x_i} < E_{x_j}$, and $E_{n_i} < E_{n_j}$ or $H_{e_i} < H_{e_j}$, A_j averagely dominates A_i.

5. Experimental Results

Our route assessment model is used in a complex route assessment system. Experiments are conducted using real terrain data with resolution 90 m × 90 m per pixel, overlaying threat zone and synthetic no-fly zone data. Alternative routes are obtained from route planner in different environments. In the following pictures, flag and triangle represent start position and destination position. In all experiments, route sample step set as $\Delta R = 420$ m, and UAV flying speed is 260 m/s.

5.1. Route's Survivability. As Figure 9(a) shows, threat A represents the perceived ADU. The curve between the start position and the destination position is a preplanned route that the UAV will fly. Monte Carlo simulations are carried out to get the survival probability when UAV traveling this route. The appearance of the first pop-up threat is generated according to the initiation function. The second and third pop-up threat is generated based on the update function of Markov model.

Figure 9(a) presents the survivability for every 42 Km along a route in one of the simulations. As can be observed, the UAV has not passed through any threat before the first discrete point, and the survivability of UAV is 100%, as the UAV near the second discrete point, it enters the affective range of the first pop-up ADU and its survivability is reduced to 82%. As the UAV flying, the second pop-up threat and

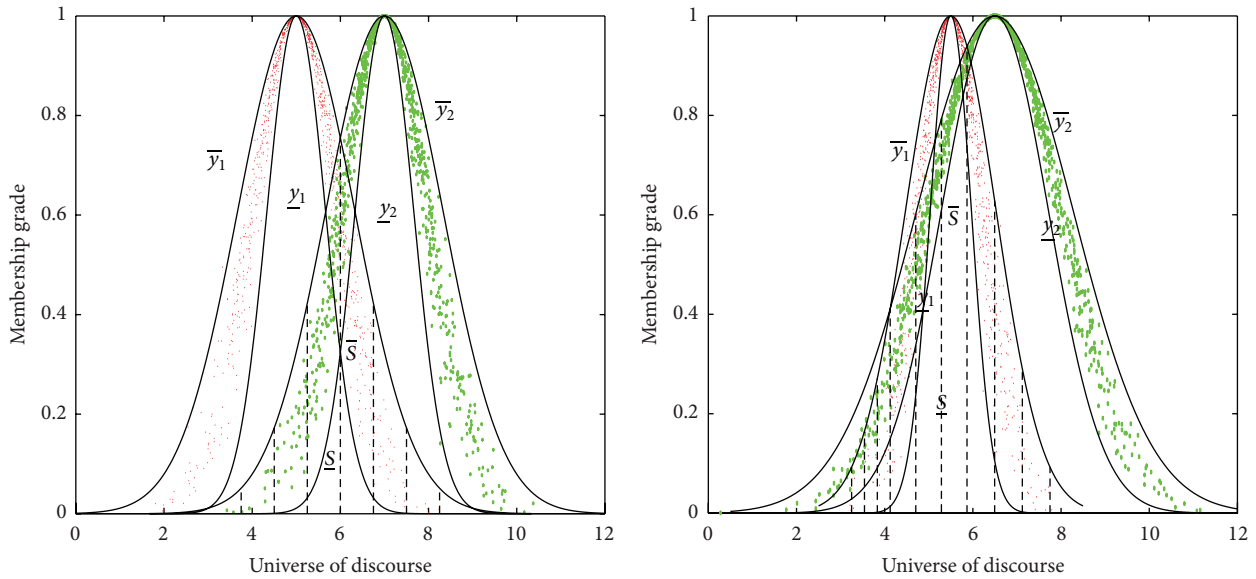

FIGURE 8: Similarity between two normal clouds based on the interaction area, upper and lower cloud curves: (a) there is one intersection point located in $[E_x - 3E_n, E_x + 3E_n]$; (b) there are two intersection points located in $[E_x - 3E_n, E_x + 3E_n]$.

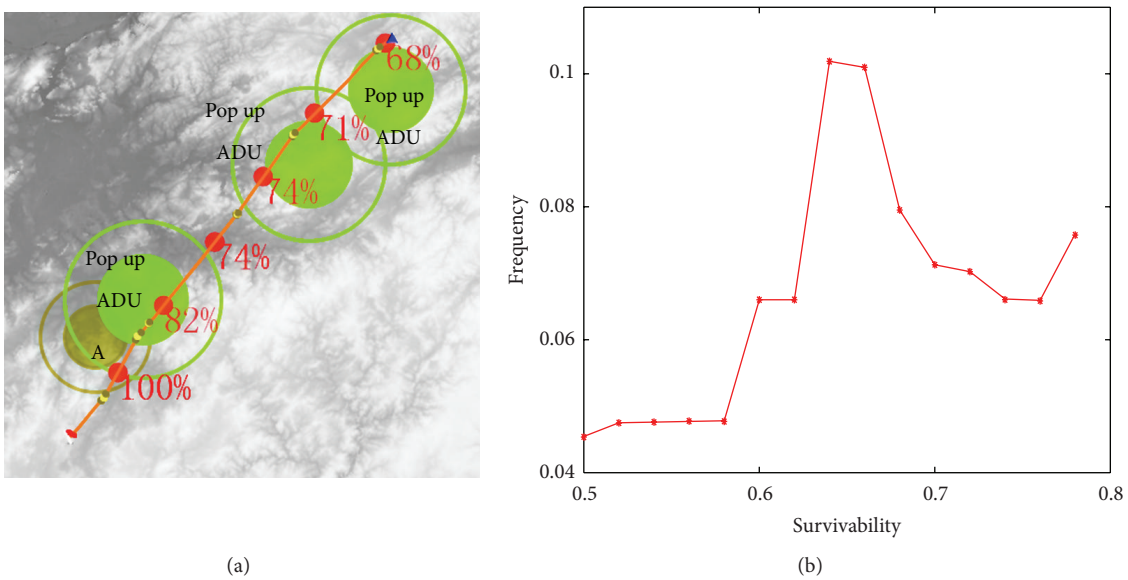

FIGURE 9: Survivability analysis of the route: (a) survivability of the discrete points on the route; (b) survivability histogram at the destination position of the route illustrated in Figure 9(a).

the third pop-up threat reduce the survivability from 74% to 71% then to 68%. When the UAV is near the destination, its survivability is reduced to 68%.

Results from Monte Carlo simulations are summarized into a histogram that can be further used to estimate UAV's survivability probability density function (see Figure 9(b)). It should be noted that shapes of the histograms are different with different numbers of pop-up threats and different threat capacities.

5.2. Route Assessment Using Normal Clouds. To illustrate our proposed approach, a typical example is selected. As shown in Figure 10, there are four no-fly zones and six perceived ADUs in the battlefield. Assume that there are three pop-up ADUs during each flight. Three preplanned UAV routes A_1, A_2, and A_3 will be evaluated and ranked, each with different characteristics. For example, route A_1 is the shortest of the three but is in an area populated by high-lethality threat zones. Route A_2 is in a less hazardous threat environment

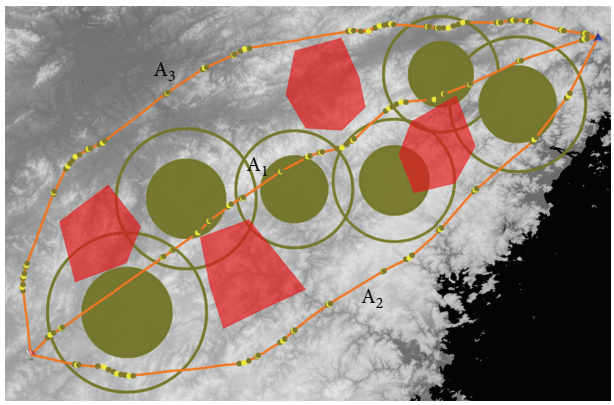

Figure 10: The battlefield environment and three candidate routes A_1, A_2, and A_3.

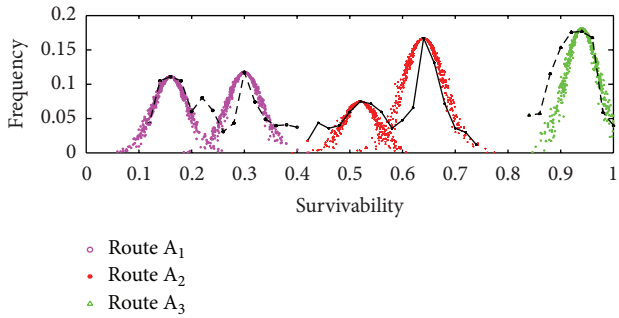

Figure 11: Survivability histograms of routes A_1, A_2, and A_3 at the destination position and their corresponding representative clouds transformed from histograms.

Table 2: Performance data of three alternate routes.

Items	J_{111} (Km)	J_{112} (rad)	J_{121} (m^2)	J_{122}	J_{123} (m)	J_3
A_1	684.17	7.57	120078	0.95	796	0.87
A_2	747.39	15.35	86219	0.90	920	0.90
A_3	807.72	18.90	137641	1.00	602	0.84

and is longer than route A_1, whereas route A_3 is in a safest environment at the expense of longest length. Therefore, selection of the optimal route should be based on mission requirements for real applications.

Performance data of these three routes is recorded in Table 2, and survivability histograms of these routes from Monte Carlo simulations are shown in Figure 11.

Figure 11 also shows the results of cloud transformation. Survivability histograms of the three routes are converted into $0.502\widetilde{S}_{11}(0.301, 0.032, 0.004) + 0.498\widetilde{S}_{12}(0.160, 0.035, 0.003)$, $0.561\widetilde{S}_{21}(0.641, 0.042, 0.004) + 0.439\widetilde{S}_{22}(0.520, 0.033, 0.003)$, and $\widetilde{S}_3(0.940, 0.033, 0.004)$, respectively.

Figure 11 reveals that skeletons of cloud drops fit with the histograms well, preserving the information contained in the histograms effectively. Data uncertainty associated with survivability is looked as integration of several normal clouds, which does not require membership functions and is simple to describe.

Table 3: Numerical characteristics and ratings of the normal clouds shown in Figures 12(a) and 12(b).

Items		$\widetilde{A}_1$	$\widetilde{A}_2$	$\widetilde{A}_3$
Cloud	a	(3.63, 0.43, 0.05)	(7.25, 0.70, 0.07)	(5.43, 0.57, 0.06)
	b	(3.67, 0.41, 0.04)	(7.25, 0.67, 0.07)	(5.42, 0.54, 0.06)
Rating	a	Marginal	Good	Adequate
	b	Marginal	Good	Adequate

Weights of criterions and subcriterions are supplied by expert's opinion, which are linguistic terms extracted from the weight sets, represented by a fuzzy weight vector:

$$W_1 = \begin{bmatrix} J_1 & J_2 & J_3 & J_{11} & J_{12} & J_{111} & J_{112} & J_{121} & J_{122} & J_{123} \\ \widetilde{1} & \widetilde{7} & \widetilde{5} & \widetilde{3} & \widetilde{7} & \widetilde{3} & \widetilde{9} & \widetilde{1} & \widetilde{9} & \widetilde{3} \end{bmatrix}. \quad (16)$$

Based on Table 2 and the collective weight vector, W_1, the aggregated normal cloud of each route is calculated. As Figure 12(a) shows, overall scores of the three routes are represented by normal clouds $\widetilde{A}_1(3.63, 0.431, 0.054)$, $\widetilde{A}_2(7.25, 0.701, 0.065)$, and $\widetilde{A}_3(5.43, 0.571, 0.061)$, respectively.

According to the proposed similarity measure (formula (15)), the similar values between the resultant assessment clouds and the standard assessment clouds labeled in Table 1 are calculated. Selecting the most similar one among all results, the overall scores are mapped into normal clouds $\widetilde{3}$, $\widetilde{7}$, and $\widetilde{5}$, respectively, and, therefore, overall performances of the three routes A_1, A_2, A_3 can be linguistically described as "Marginal," "Excellent," and "Good," respectively. Ranking order of the three routes is $\widetilde{A}_2 \succ \widetilde{A}_3 \succ \widetilde{A}_1$.

To investigate the effects of random uncertainty in survivability on the on the overall performances, we represent assessments of combat survival by expected values of survivability probability histograms in this experiment. With the same weight vector W_1, the overall aggregated results are obtained, depicted in Figure 12(b). The ranking order is also $\widetilde{A}_2 \succ \widetilde{A}_3 \succ \widetilde{A}_1$. Comparing Figures 12(a) and 12(b), it can be observed that the cloud drops spread out over a larger range of values generally.

Table 3 summarizes the aggregated results in Figures 12(a) and 12(b). As can be observed, the expectation of each normal cloud shown in Figure 12(a) is almost the same as its counterpart shown in Figure 12(b). However, entropy E_n and super entropy H_e increase, reflecting the additional random uncertainty regarding the dynamic battlefield environment.

Table 4 records the similarities among $\widetilde{A}_1$, $\widetilde{A}_2$, and $\widetilde{A}_3$ depicted in Figures 12(a) and 12(b). Observe that the similarity between $\widetilde{A}_2$ and $\widetilde{A}_3$ shown in Figure 12(a) is 0.113, and, therefore, the confidence level in selecting A_2 as the best one is 88.7%, whereas the similarity between $\widetilde{A}_2$ and $\widetilde{A}_3$ shown in Figure 12(b) is 0.098. Consequently, one may be less certain about choosing route A_2 as the winner when there is uncertainty regarding the dynamic battlefield environment than when there is no random uncertainty in the battlefield.

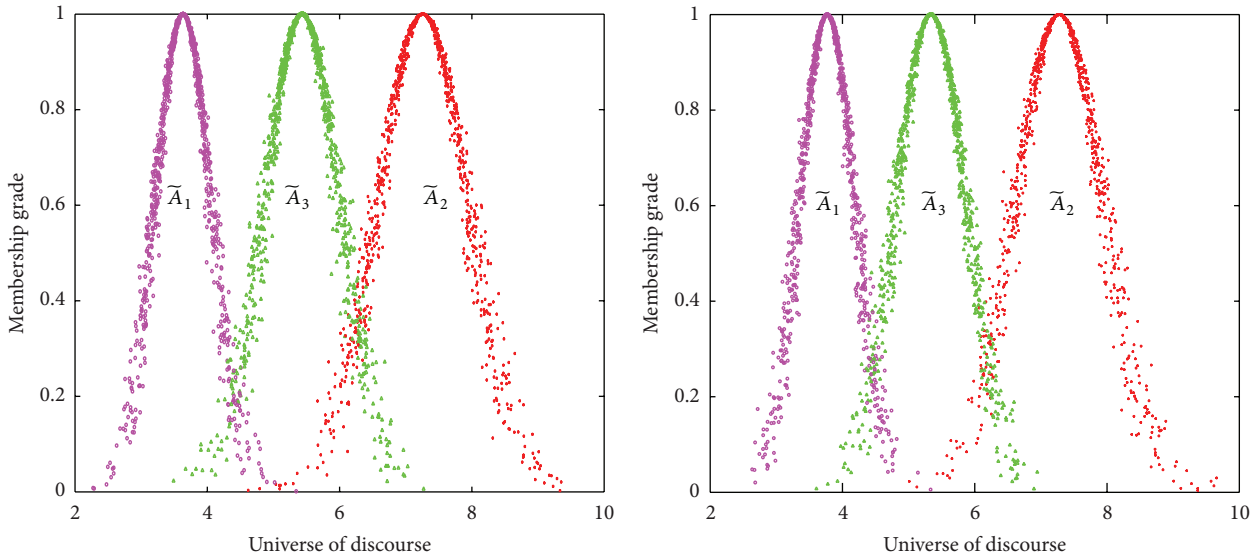

Figure 12: Comparison of the overall clouds with different descriptions of scores on combat survival: (a) overall clouds when scores on combat survival are represented by clouds generated from histograms; (b) overall clouds when scores on combat survival are represented by the expected values.

Table 4: Similarities among the normal clouds shown in Figures 12(a) and 12(b).

Items	$\widetilde{A}_1$		$\widetilde{A}_2$		$\widetilde{A}_3$	
	a	b	a	b	a	b
$\widetilde{A}_1$	1.00	1.00	0.00	0.00	0.066	0.059
$\widetilde{A}_2$	0.00	0.00	1.00	1.00	0.113	0.098
$\widetilde{A}_3$	0.066	0.059	0.113	0.098	1.00	1.00

5.3. Comparisons with Other Approaches. As previously mentioned, in the area of route assessment, most of the studies employed weighted average (WA) method to aggregate scores of criteria, where all weights and scores of criteria are fixed numbers [2–7]. Several studies employed T1 FSs to represent the linguistic variables and vague patterns in the route assessment problems. In this section, the proposed method is compared with the weighted average method and the assessment method using T1 FSs [9, 10]. As mentioned before, selection of the optimal route should be based on expert preferences and mission conditions. The overall results and ranking order can be dependent on the weight vector. To demonstrate characteristics of route assessment problem and the feasibility of the proposed method, in this experiment, experts' preferences over multiple assessment criteria are represented by weight vector W_2, expressed by

$$W_2 = \begin{bmatrix} J_1 & J_2 & J_3 & J_{11} & J_{12} & J_{111} & J_{112} & J_{121} & J_{122} & J_{123} \\ \widetilde{9} & \widetilde{5} & \widetilde{1} & \widetilde{7} & \widetilde{1} & \widetilde{3} & \widetilde{9} & \widetilde{1} & \widetilde{9} & \widetilde{3} \end{bmatrix}. \quad (17)$$

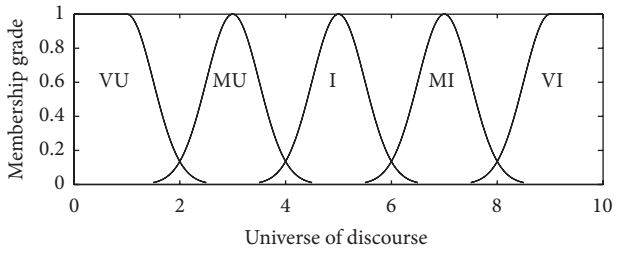

Figure 13: Linguistic variables and their corresponding T1 FSs.

In the weighted average method, all weights and scores of assessment criteria are real numbers, and score on combat survival is represented by the expected value of survivability probability histogram. The calculated ranking order is $\widetilde{A}_1 \succ \widetilde{A}_2 \succ \widetilde{A}_3$ and route A_1 is the best one. The weighted average algorithm, probably the most widely used form of aggregation in MCDM problems, is easy to compute and understand. However, uncertainties are not addressed and incorporated in the overall assessment results.

In the T1 FSs based assessment method, all words concerning weights of assessment criteria are modeled by T1 FSs. Figure 13 shows the linguistic terms (VU, MU, I, MI, VI) for representing importance of criterions and their corresponding T1 FSs. It can be noticed that randomness of membership degree is not managed. As Figure 14(a) demonstrates, the aggregated overall results are also T1 FSs by using the computing with words (CWW) engine [39], and the ranking order is $\widetilde{A}_1 \succ \widetilde{A}_2 \succ \widetilde{A}_3$.

With such a route assessment method based on cloud model, fuzziness and randomness of linguistic variables are integrated to model expert knowledge, and assessments of combat survival are expressed by normal clouds. Therefore,

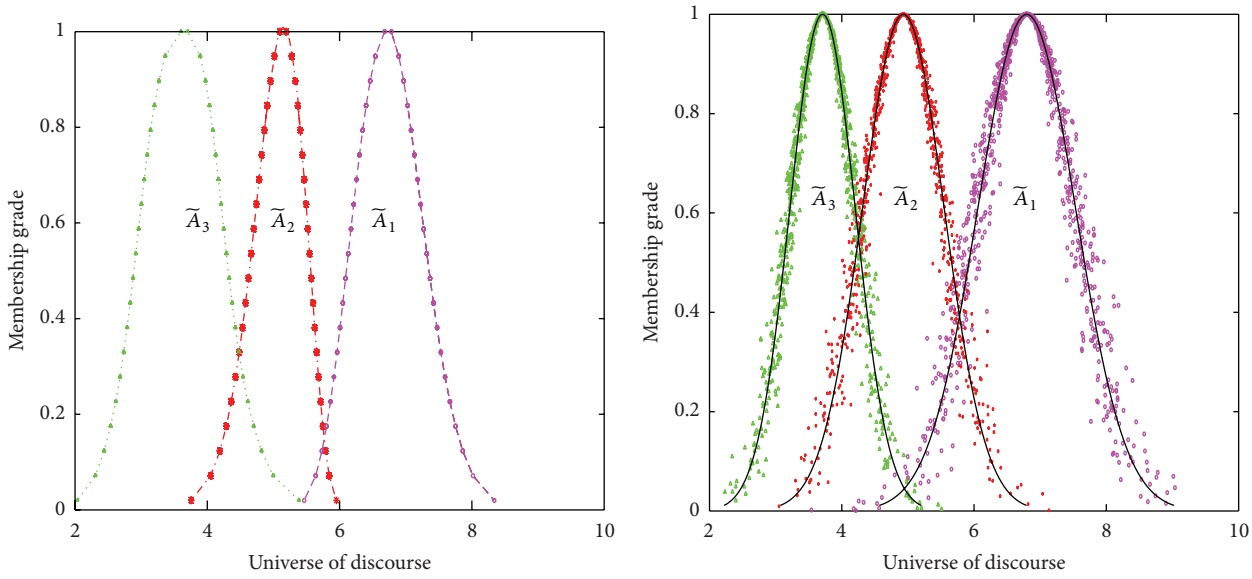

Figure 14: Comparisons of overall results provided by T1 FSs based assessment method and the proposed method: (a) aggregated total results provided by T1 FSs based assessment method; (b) aggregated total results provided by the proposed method.

Table 5: Aggregated results provided by the three methods.

Method	$\widetilde{A}_1$	$\widetilde{A}_2$	$\widetilde{A}_3$
WA	6.73	5.14	3.65
T1 FSs	6.78	4.95	3.64
CM	(6.64, 0.94, 0.10)	(5.13, 0.62, 0.07)	(3.71, 0.50, 0.06)

both fuzziness and randomness are managed and embodied in the final results. As Figure 14(b) reveals, the final results are cloud graphs that are more intuitive, effective, and understandable than T1 FSs. The final ranking order is $\widetilde{A}_1 \succ \widetilde{A}_2 \succ \widetilde{A}_3$, consistent with the results provided by the above two methods. Table 5 shows the aggregated results of the weighted average method, centroids of the aggregated results produced by the T1 FSs based assessment method, and the normal clouds obtained from the proposed method.

From Table 5, it can be observed that there are few differences among the resultant ranks provided by the three assessment methods. Compared with traditional methods of route assessment, the proposed method can manage various kinds and sources of uncertainties, including randomness, fuzziness, and their interrelationship, and produce good results that can provide the decision makers useful and informative decision references. Comparing Figures 12(a) and 14(b), we can observe that the final rankings are different with different weight vectors: in Figure 12(a), route A_2 ranks highest, whereas in Figure 14(b), route A_1 ranks highest. This is because the final results depend on the assessment results of the route in a series of subcriterions and the weight vector. For example, route A_1 is the shortest and smoothest of all and the criterion considered is mainly flight safety in Figure 14(b), and therefore, A_1 ranks highest in Figure 14(b). Therefore, we can conclude that the final solutions provided by the proposed method are in accordance with mission scenarios and human preferences. The proposed method can provide a framework to assist decision makers in evaluating route alternatives and making an objective route selection.

6. Conclusion

A route assessment method based on cloud model that enables experts to assess different candidate routes and find an optimal one is proposed in this paper. A systematic assessment framework that incorporates computational models for quantifying and propagating route criterions is established. The systems-based multilevel architecture of the assessment framework is extremely flexible and would easily allow users to replace or add specific modules with updated ones that reflect needed levels of analysis sophistication. Random uncertainty associated with pop-up threats is modeled by Markov chain and estimate of survivability probability density function is obtained from Monte Carlo simulations. Therefore, random uncertainty in the battlefield is effectively represented.

Because route assessment is not an exact process and has fuzziness in its body, here, the usage of cloud model to deal with linguistic uncertainty makes the application realistic and reliable. Cloud transformation is introduced to convert each individual survivability histogram into normal clouds, effectively keeping the information in the survivability histogram. With the arithmetic operation, different kinds of uncertainties existing in the data are effectively preserved and propagated into the final assessment. As the results demonstrate in the application examples, it is found that the proposed similarity measure taking account both shape and

thickness information of cloud drops is practical for ranking route alternatives in terms of their overall performances.

The proposed route assessment approach provides a general guideline for assessment problems where different kinds of uncertainties such as randomness and fuzziness exist. Meanwhile, we believe that there is room for future enhancements and validations of the approach presented. For example, how to extend the current approach to deal with the inherent uncertainty and imprecision of the human decision making process should be examined. This may be improved in future developments.

Conflict of Interests

The authors declare that there is no conflict of interests regarding the publication of this paper.

References

[1] M. Peschel and R. R. Murphy, "On the human-machine interaction of unmanned aerial system mission specialists," *IEEE Transactions on Human-Machine Systems*, vol. 43, no. 1, pp. 53–62, 2013.

[2] C. Zheng, L. Li, F. Xu, F. Sun, and M. Ding, "Evolutionary route planner for unmanned air vehicles," *IEEE Transactions on Robotics*, vol. 21, no. 4, pp. 609–620, 2005.

[3] M. L. Cummings, J. J. Marquez, and N. Roy, "Human-automated path planning optimization and decision support," *International Journal of Human Computer Studies*, vol. 70, no. 2, pp. 116–128, 2012.

[4] J. J. Ruz, O. Arévalo, G. Pajares, and J. M. de La Cruz, "Decision making among alternative routes for UAVs in dynamic environments," in *Proceedings of the 12th IEEE International Conference on Emerging Technologies and Factory Automation (ETFA '07)*, pp. 997–1004, September 2007.

[5] X. Liu, C. Zhou, and M. Ding, "3D multipath planning for UAV based on network graph," *Journal of Systems Engineering and Electronics*, vol. 22, no. 4, pp. 640–646, 2011.

[6] V. Roberge, M. Tarbouchi, and G. Labonte, "Comparison of parallel genetic algorithm and particle swarm optimization for real-time UAV path planning," *IEEE Transactions on Industrial Informatics*, vol. 9, no. 1, pp. 132–141, 2013.

[7] E. Besada-Portas, L. de La Torre, J. M. de La Cruz, and B. de Andrés-Toro, "Evolutionary trajectory planner for multiple UAVs in realistic scenarios," *IEEE Transactions on Robotics*, vol. 26, no. 4, pp. 619–634, 2010.

[8] L. A. Zadeh, "Quantitative fuzzy semantics," *Information Sciences*, vol. 3, no. 2, pp. 159–176, 1971.

[9] R. Kala, A. Shukla, and R. Tiwari, "Fusion of probabilistic A∗ algorithm and fuzzy inference system for robotic path planning," *Artificial Intelligence Review*, vol. 33, no. 4, pp. 307–327, 2010.

[10] M. A. P. Garcia, O. Montiel, O. Castillo, R. Sepúlveda, and P. Melin, "Path planning for autonomous mobile robot navigation with ant colony optimization and fuzzy cost function evaluation," *Applied Soft Computing Journal*, vol. 9, no. 3, pp. 1102–1110, 2009.

[11] D. Li, D. Cheung, X. Shi, and V. Ng, "Uncertainty reasoning based on cloud models in controllers," *Computers and Mathematics with Applications*, vol. 35, no. 3, pp. 99–123, 1998.

[12] D. Li and Y. Du, *Artificial Intelligence with Uncertainty*, Chapman & Hall/CRC, 2007.

[13] Y. Jiang, J. Jiang, and Y. Zhang, "A novel fuzzy multiobjective model using adaptive genetic algorithm based on cloud theory for service restoration of shipboard power systems," *IEEE Transactions on Power Systems*, vol. 27, no. 2, pp. 612–620, 2012.

[14] C. Dai, W. Chen, and Y. Zhu, "Seeker optimization algorithm for digital IIR filter design," *IEEE Transactions on Industrial Electronics*, vol. 57, no. 5, pp. 1710–1718, 2010.

[15] J. Zhang, J. Tang, and F. Pei, "A method for network security risk assessment and decision-making based on the cloud model," *Journal of Convergence Information Technology*, vol. 7, no. 6, pp. 146–153, 2012.

[16] Z. Zhou, "Cognition and removal of impulse noise with uncertainty," *IEEE Transactions on Image Processing*, vol. 21, no. 7, pp. 3157–3167, 2012.

[17] T. J. Ross, J. M. Booker, and A. C. Montoya, "New developments in uncertainty assessment and uncertainty management," *Expert Systems with Applications*, vol. 40, no. 3, pp. 964–974, 2013.

[18] T. Wu and K. Qin, "Comparative study of image thresholding using type-2 fuzzy sets and cloud model," *International Journal of Computational Intelligence Systems*, vol. 3, supplement 1, pp. 61–73, 2010.

[19] J. Karimi and S. H. Pourtakdoust, "Optimal maneuver-based motion planning over terrain and threats using a dynamic hybrid PSO algorithm," *Aerospace Science and Technology*, vol. 26, no. 1, pp. 60–71, 2013.

[20] Y. Liu, J. B. Cruz, and C. J. Schumacher, "Pop-up threat models for persistent area denial," *IEEE Transactions on Aerospace and Electronic Systems*, vol. 43, no. 2, pp. 509–521, 2007.

[21] A. Schulte, "Mission management and crew assistance for military aircraft-cognitive concepts and prototype assessment," Tech. Rep. RTO-ENP-019, ESG- Elektroniksystem -und Logistik -GmbH Advanced Avionics Systems, 2001.

[22] S. M. Malaek and A. R. Kosari, "Dynamic based cost functions for TF/TA flights," *IEEE Transactions on Aerospace and Electronic Systems*, vol. 48, no. 1, pp. 44–63, 2012.

[23] R. Samar and A. Rehman, "Autonomous terrain-following for unmanned air vehicles," *Mechatronics*, vol. 21, no. 5, pp. 844–860, 2011.

[24] L. de Filippis, G. Guglieri, and F. Quagliotti, "A minimum risk approach for path planning of UAVs," *Journal of Intelligent & Robotic Systems*, vol. 61, no. 1–4, pp. 203–219, 2011.

[25] X. Zhang, J. Chen, B. Xin, and H. Fang, "Online path planning for UAV using an improved differential evolution algorithm," in *Proceeding of the 8th World Congress of the International Federation of Automatic Control*, pp. 6349–6354, Milano, Italy, September 2011.

[26] S. Nair and M. Kobilarov, "Collision avoidance norms in trajectory planning," in *Proceedings of the American Control Conference (ACC '11)*, pp. 4667–4672, San Francisco, Calif, USA, July 2011.

[27] I. K. Nikolos, E. S. Zografos, and A. N. Brintaki, "UAV path planning using evolutionary algorithms," in *Innovations in Intelligent Machines*, vol. 70 of *Studies in Computational Intelligence*, pp. 77–111, 2007.

[28] T. Erlandsson and L. Niklasson, "An air-to-ground combat survivability model," *The Journal of Defense Modeling and Simulation: Applications, Methodology, Technology*, 2013.

[29] Y. Shi, A. Zhang, X. Gao, and Z. Tan, "Cloud model and its application in effectiveness evaluation," in *Proceedings of the International Conference on Management Science and Engineering 15th Annual Conference (ICMSE '08)*, pp. 250–255, Long Beach, Calif, USA, September 2008.

[30] L. Li, L. Liu, C. Yang, and Z. Lia, "The comprehensive evaluation of smart distribution grid based on cloud model," *Energy Procedia*, vol. 17, pp. 96–102, 2012.

[31] C.-B. Li, Z.-Q. Qi, and X. Feng, "A multi-risks group evaluation method for the informatization project under linguistic environment," *Journal of Intelligent & Fuzzy Systems*, vol. 26, no. 3, pp. 1581–1592, 2014.

[32] Y. Xiaojun, Y. Liaoliao, P. Hui et al., "Encoding words into Cloud models from interval-valued data via fuzzy statistics and membership function fitting," *Knowledge and Information Systems*, vol. 55, pp. 114–124, 2014.

[33] X. Yang, L. Yan, and L. Zeng, "How to handle uncertainties in AHP: the Cloud Delphi hierarchical analysis," *Information Sciences*, vol. 222, pp. 384–404, 2013.

[34] Z. Jie, J.-A. Zhang, and J. Wen, "Trust evaluation model based on cloud model for C2C electronic commerce," in *Proceedings of the International Conference on Computer Application and System Modeling (ICCASM '10)*, pp. V8-506–V8-509, October 2010.

[35] L. Tao, D. Huang, and L. Hong, "Research on subjective trust model based on cloud model for open networks," *Journal of Computational Information Systems*, vol. 7, no. 13, pp. 4844–4854, 2011.

[36] J. Dai, Z. He, and F. Hu, "Reduction algorithm for incomplete decision table with continuous attributes based on cloud model," *Journal of Computational Information Systems*, vol. 7, no. 5, pp. 1722–1729, 2011.

[37] H. Lu, E. Pi, Q. Peng, L. Wang, and C. Zhang, "A particle swarm optimization-aided fuzzy cloud classifier applied for plant numerical taxonomy based on attribute similarity," *Expert Systems with Applications*, vol. 36, no. 5, pp. 9388–9397, 2009.

[38] H. Li and C. Guo, "Piecewise cloud approximation for time series mining," *Knowledge-Based Systems*, vol. 24, no. 4, pp. 492–500, 2011.

[39] D. Wu and J. M. Mendel, "Computing with words for hierarchical decision making applied to evaluating a weapon system," *IEEE Transactions on Fuzzy Systems*, vol. 18, no. 3, pp. 441–460, 2010.